

A Novel Precoder for Peak-to-Average Power Ratio Reduction in OTFS Systems

Saurabh Prakash, Venkatesh Khammammetti and Saif Khan Mohammed, *Senior Member, IEEE*

Abstract—We consider the issue of high peak-to-average-power ratio (PAPR) of Orthogonal time frequency space (OTFS) modulated signals. This paper proposes a low-complexity novel iterative PAPR reduction method which achieves a PAPR reduction of roughly 5 dB when compared to a OTFS modulated signal without any PAPR compensation. Simulations reveal that the PAPR achieved by the proposed method is significantly better than that achieved by other state-of-art methods. Simulations also reveal that the error rate performance of OTFS based systems with the proposed PAPR reduction is similar to that achieved with the other state-of-art methods.

Index Terms—Orthogonal time frequency space modulation, Delay-Doppler domain, Peak-to-average power ratio.

I. INTRODUCTION

Next generation communication systems are envisaged to support high throughput and reliable communication even for high mobility scenarios (e.g., aircraft/UAV communications, high speed train, etc) [1]. The performance of Orthogonal Frequency Division Multiplexing (OFDM) based systems used in 4G/5G systems is known to degrade severely in high mobility scenarios due to the high channel Doppler shift [2].

Recently introduced Orthogonal Time Frequency Space (OTFS) modulation has been shown to be robust to mobility induced Doppler spread [3]–[6]. In OTFS modulation, information symbols are embedded in the delay-Doppler (DD) domain and therefore detection [7]–[9] and channel estimation [10]–[13] are also carried out in the DD domain. A collection of literature on OTFS is available in [14].

In an OTFS transmitter, the information symbols are first converted to time-frequency (TF) domain symbols which are then converted to time-domain (TD) transmit signal using an OFDM modulator. Due to this transformation from information symbols to TD transmit signal, the peak-to-average-power ratio (PAPR) of the transmit TD signal can be large [16]. Due to large PAPR, linear power amplifiers (PA) must be used to avoid signal distortion. Linear PAs are however power inefficient (the radiated power is a small fraction of the total power input to the PA) which reduces the overall energy efficiency [15].

Saurabh Prakash and Saif Khan Mohammed are with the Department of Electrical Engineering, Indian Institute of Technology Delhi, India (E-mail: Saurabh.Prakash@ee.iitd.ac.in, saifkhanmohammed@gmail.com). S. K. Mohammed is also associated with Bharti School of Telecom. Technology and Management (BSTTM), IIT Delhi. Venkatesh Khammammetti is with the Department of Electrical and Computer Engineering, Duke University, USA (E-mail: venkatesh.khammammetti@gmail.com). The work of S. K. Mohammed was supported by the Jai Gupta Chair at I.I.T. Delhi.

This work has been submitted to the IEEE for possible publication. Copyright may be transferred without notice, after which this version may no longer be accessible.

PAPR of OFDM modulated signals is known to be high and for which several PAPR reduction methods have been proposed in prior literature [17]. In comparison to OFDM, since OTFS is a relatively recent waveform there are some works reported on PAPR reduction for OTFS modulated signals [18]–[20].

In this paper, we propose a novel PAPR reduction method for OTFS based systems when PSK information symbols are used. The main contributions of this paper are:

- The proposed method precodes each information symbol by modifying its amplitude (without changing the phase/angle which carries information) in such a way that it helps in reducing the PAPR of the corresponding transmit TD signal (see Section III).
- In Section IV we study the complementary cumulative distribution function (CCDF) of the PAPR, for an OTFS system where no measures are taken to reduce PAPR (i.e., referred to as an uncompensated system), for the proposed method and for the other state-of-art methods in [18]–[20]. Simulations reveal that the proposed PAPR reduction method achieves significant PAPR reduction of roughly 5 dB when compared to an uncompensated system. Further, the proposed method has lower complexity and smaller PAPR when compared to the other state-of-art methods in [18]–[20].
- In Section IV we also study the error rate performance of the proposed method which reveals that it achieves similar performance as that achieved with the DFT-precoded method (in [19]) and the clipping and filtering based method (in [20]). The proposed method achieves better error-rate performance than the companding based method (in [18]). Also, the invariance of the error rate performance of OTFS systems to a wide range of channel Doppler spread is valid even when the transmit signal is based on the proposed PAPR reduction.

II. SYSTEM MODEL

In this paper, we consider an OTFS based wireless communication system with a single antenna base station (BS) and a single antenna user terminal (UT). In OTFS modulation, the information symbols are embedded in the delay-Doppler (DD) domain. OTFS modulation is described in detail in [3] and is parameterized by $T > 0$, and positive integers M, N . Let $x[k, l]$, $k = 0, \dots, N - 1, l = 0, \dots, M - 1$ denote the MN DD domain information symbols. The information symbols belong to a D -ary PSK alphabet set $\mathcal{S}_{A,D} = \{A e^{j2\pi \frac{p}{D}} \mid p = 0, 1, \dots, D-1\}$. By using the inverse symplectic finite Fourier

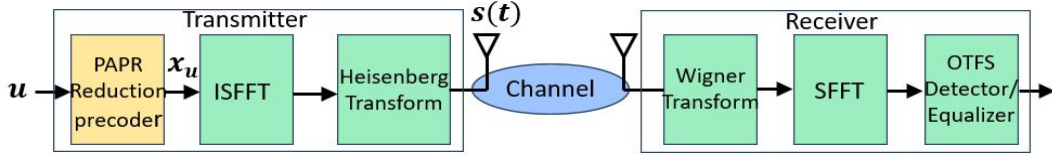


Fig. 1. Zak-OTFS transceiver signal processing with proposed precoding at transmitter for PAPR reduction.

transform (ISFFT), the DD domain information symbols are transformed to time-frequency (TF) symbols given by

$$X[n, m] = \sum_{k=0}^{N-1} \sum_{l=0}^{M-1} x[k, l] e^{-j2\pi(\frac{ml}{M} - \frac{nk}{N})}$$

$$n = 0, 1, \dots, N-1, \quad m = 0, 1, \dots, M-1. \quad (1)$$

The time-frequency symbols are then converted to the transmit time domain signal $s(t)$ using the Heisenberg transform, i.e.

$$s(t) = \sum_{n=0}^{N-1} \sum_{m=0}^{M-1} X[n, m] g_{tx}(t - nT) e^{j2\pi m \Delta f (t - nT)} \quad (2)$$

where $g_{tx}(t)$ is the transmit pulse and $\Delta f = \frac{1}{T}$. In this paper we consider the rectangular transmit pulse, i.e.

$$g_{tx}(t) = \begin{cases} \frac{1}{\sqrt{T}} & , 0 \leq t < T \\ 0 & , \text{otherwise} \end{cases}. \quad (3)$$

The duration of $s(t)$ is NT seconds and has a bandwidth of $M\Delta f$ Hz.

A. Sampling the TD transmit signal

The transmit signal $s(t)$ is sampled at a sampling rate equal to the bandwidth $M\Delta f$ resulting in the MN discrete-time samples

$$s[n] \triangleq s\left(t = \frac{n}{M\Delta f}\right), \quad n = 0, 1, \dots, MN-1. \quad (4)$$

Consider the vector of discrete-time transmit samples, $\mathbf{s} \in \mathbb{C}^{MN}$ whose i -th element is $s[i-1]$, $i = 1, 2, \dots, MN$. From [21] it follows that

$$\mathbf{s} = (\mathbf{F}_N^H \otimes \mathbf{I}_M) \mathbf{x} \quad (5)$$

where $\mathbf{x} \in \mathbb{C}^{MN}$ is the vector of the MN DD domain information symbols whose $(kM+l+1)$ -th element is $x[k, l]$, $k = 0, 1, \dots, N-1, l = 0, 1, \dots, M-1$. Further, \mathbf{F}_N denotes the $N \times N$ DFT matrix whose element in its p -th row and q -th column is $e^{j2\pi pq/N}$, $p, q = 0, 1, \dots, N-1$. Also \mathbf{I}_M denotes the $M \times M$ identity matrix and \otimes denotes Kronekar product for matrices.

III. PROPOSED NOVEL APPROACH FOR PAPR COMPENSATION

Peak to Average Power ratio (PAPR) is the ratio of maximum transmit power to the average transmit power in an OTFS frame and it is given by

$$\text{PAPR}(\mathbf{s}) = \frac{\max_{n=0, \dots, MN-1} |s[n]|^2}{\frac{1}{MN} \sum_{n=1}^{MN} |s[n]|^2} = \frac{MN \|\mathbf{s}\|_\infty^2}{\|\mathbf{s}\|_2^2}. \quad (6)$$

In the proposed PAPR compensation method, for a given block of MN information symbols, $k = 0, 1, \dots, N-1$, $l = 0, 1, \dots, M-1$, we precode them into precoded information symbols $x[k, l]$ which are then transmitted using (1) and (2). The information symbols $u[k, l]$ belong to the regular D -ary PSK alphabet set $\mathcal{S}_{A,D}$. However, the precoded information symbols belong to the extended alphabet set $\mathcal{S} = \mathcal{S}_{A,D} \cup \mathcal{S}_{2A,D}$. To be precise, for the (k, l) -th information symbol $u[k, l] \in \mathcal{S}_{A,D}$, the corresponding precoded (k, l) -th symbol $x[k, l]$ can be either $u[k, l]$ or $2u[k, l]$. In PSK, information bits are encoded into the angle of the complex symbol. Since the angle of $u[k, l]$ and $2u[k, l]$ is the same, information is preserved (see illustration in Fig. 2).

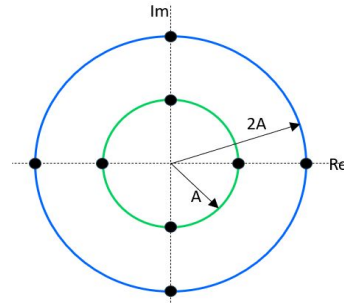


Fig. 2. $D = 4$. Alphabet set $\mathcal{S}_{A,D}$ (black dots on the green circle) and $\mathcal{S}_{2A,D}$ (black dots on the blue circle). Precoded symbols belong to the extended alphabet set $\mathcal{S}_{A,D} \cup \mathcal{S}_{2A,D}$ (consisting of all eight black dots on both circles).

Consider a given block of MN information symbols $u[k, l]$ denoted by an information symbol vector $\mathbf{u} \in (\mathcal{S}_{A,D})^{MN}$. For a given \mathbf{u} consider the set of 2^{MN} vectors

$$\mathcal{B}(\mathbf{u}) \triangleq \left\{ \mathbf{x} \in \mathcal{S} \mid x[i] = u[i] \text{ or } 2u[i], i = 1, 2, \dots, MN \right\} \quad (7)$$

In the proposed method we choose the precoded vector \mathbf{x} to be the one which minimizes PAPR. For a given \mathbf{u} , we denote the chosen \mathbf{x} by \mathbf{x}_u which is given by

$$\mathbf{x}_u \triangleq \arg \min_{\mathbf{x} \in \mathcal{B}(\mathbf{u})} \text{PAPR}((\mathbf{F}_N^H \otimes \mathbf{I}_M) \mathbf{x}). \quad (8)$$

The block diagram of OTFS signal processing with the proposed PAPR reduction is shown in Fig. 1. The proposed method provides a way to reduce the PAPR by allowing the precoded symbols to take values over a larger alphabet set than that for the information symbols. However, since the number of possible precoded vectors 2^{MN} is large for large (M, N) , we next propose an iterative algorithm for approximately solving (8). Although this iterative method does not solve (8) exactly, it still achieves a significant PAPR improvement

compared to that for the uncompensated system (see Section IV).

The proposed iterative method takes as input the information symbol vector \mathbf{u} and outputs the precoded vector \mathbf{x}^* which is an approximation to the optimal \mathbf{x}_u in (8). Its algorithmic listing is provided below in Algorithm 1. In step-2, we initialize the precoded vector to be \mathbf{u} itself and the iteration counter $Iter$ to 0. In each iteration (from steps 4 – 16), \mathbf{x}^* denotes the best precoded vector found so far for which PAPR is p^* . Each precoded symbol in \mathbf{x}^* has amplitude either A or $2A$. In each iteration, we go through each of the MN precoded symbols in \mathbf{x}^* and modify them one at a time (see steps 4 – 8). In step-6, we scale the amplitude of the t -th precoded symbol by the factor $2^{\left(3-2\frac{|x^*[t]|}{A}\right)}$ (note that we only modify the amplitude and not the angle/phase of the symbol as it carries information). It is clear that if $|x^*[t]| = A$ then the scaling factor is 2 (i.e., the modified amplitude is $2A$) and if $|x^*[t]| = 2A$ then the scaling factor is $1/2$ (i.e., the modified amplitude is A). The PAPR with the modified precoded vector (where only one symbol is modified) is computed in step-7 and saved. In step-9, we search for the symbol (out of all MN symbols) whose modification gives the smallest PAPR. If this smallest PAPR p_{min} is less than the smallest achieved PAPR so far (i.e., p^*), then we update p^* to p_{min} and we update the symbol in \mathbf{x}^* whose modification resulted in the smallest PAPR so far (see steps 11 – 12). However, if the smallest PAPR p_{min} is not smaller than p^* then we terminate. We also terminate the algorithm if the maximum number of iterations $MaxIter$ is reached.

Algorithm 1 Proposed Iterative Method for PAPR Compensation

- 1: **Input:** Information symbol vector \mathbf{u} , alphabet sets $\mathcal{S}_{A,D}, \mathcal{S}_{2A,D}$, $stop = 0$, $MaxIter = 5$.
 - 2: **Initialization:** $\mathbf{x}^* = \mathbf{u}$. $p^* = \text{PAPR}((\mathbf{F}_N^H \otimes \mathbf{I}_M) \mathbf{u})$, $Iter = 0$.
 - 3: **repeat**
 - 4: **for** $t = 1$ to MN **do**
 - 5: $\mathbf{x} = \mathbf{x}^*$.
 - 6: $x[t] = 2^{\left(3-2\frac{|x^*[t]|}{A}\right)} x^*[t]$.
 - 7: $p[t] = \text{PAPR}((\mathbf{F}_N^H \otimes \mathbf{I}_M) \mathbf{x})$.
 - 8: **end for**
 - 9: $p_{min} = \min_{t=1,2,\dots,MN} p[t]$, $i = \arg \min_{t=1,2,\dots,MN} p[t]$.
 - 10: **if** $p_{min} < p^*$ **then**
 - 11: $x^*[i] = 2^{\left(3-2\frac{|x^*[i]|}{A}\right)} x^*[i]$.
 - 12: $p^* = p_{min}$.
 - 13: **else**
 - 14: $stop = 1$.
 - 15: **end if**
 - 16: $Iter = Iter + 1$.
 - 17: **until** ($stop = 1$ or $Iter = MaxIter$), **Output:** \mathbf{x}^*, p^* .
-

For each precoded vector \mathbf{x} , the complexity of computing the transmit time-domain vector $\mathbf{s} = (\mathbf{F}_N^H \otimes \mathbf{I}_M) \mathbf{x}$ is $O(MN \log(MN))$. The complexity of step-7 is therefore $O(MN \log(MN))$. In steps 4-8, the PAPR is computed for all vectors obtained by modifying one symbol, and hence the complexity is $O(M^2 N^2 \log(MN))$. Since the algorithm usually stops after a few iterations (less than five), the overall complexity is $O(M^2 N^2 \log(MN))$. Other simple PAPR

reduction methods like those based on companding have complexity same as that of computing the transmit time-domain vector i.e., $O(MN \log(MN))$ which is smaller than the $O(M^2 N^2 \log(MN))$ complexity of the proposed method. However, as we shall see in Section IV, the PAPR reduction achieved with the proposed method is significantly *better* than that achieved with companding or other state-of-art methods.

IV. NUMERICAL SIMULATIONS

In this section, we report the simulation results for the proposed iterative PAPR compensation method, in terms of the BER performance and the complementary cumulative distribution function (CCDF) of the time-domain transmit symbols $s[n], n = 1, 2, \dots, MN$. We also compare the CCDF and BER performance of the proposed method with that of other methods used for PAPR reduction in OTFS based systems, like companding in [18], DFT precoded OTFS in [19], and clipping and filtering based compensation in [20]. For numerically computing the CCDF we compute the PAPR for a thousand different randomly generated information vectors. In the CCDF plot, for each value x on the X-axis, the corresponding value on the Y-axis gives the empirically computed probability (using the thousand PAPR values) that the PAPR is greater than x .

The receiver processing is same as that in [3], i.e., Wigner transform of the received time-domain signal followed by Symplectic Finite Fourier Transform (SFFT) resulting in received DD domain symbols. The received DD domain symbols can be expressed as the sum of a DD domain noise vector and the signal vector which is the product of an effective DD domain channel matrix and the vector of precoded symbols \mathbf{x} [13]. Minimum Mean Square Error Estimation (MMSE) based equalization gives an estimate of each of the MN precoded symbol. The information bits modulated onto each information symbol are then estimated from the angle/phase of the corresponding estimated precoded symbol at the output of the MMSE equalizer.

We consider OTFS based systems with $\Delta f = 1/T = 15\text{KHz}$, $M = 16$, $N = 16$ and a carrier frequency of $f_c = 2\text{GHz}$. The 3GPP Extended Typical Urban (ETU 300) channel model is considered, with a maximum Doppler shift of $\nu_{\max} = 300$ Hz. There are nine channel paths and the delay profile is $[0, 50, 120, 200, 230, 500, 1600, 2300, 5000]$ ns, while the relative power profile is $\mathbf{P} = [-1, -1, -1, 0, 0, 0, -3, -5, -7]$ dB. The channel path gains $h_i, i = 1, 2, \dots, 9$ are modeled as i.i.d. zero mean Rayleigh random variables having variance whose ratio is as per the power profile (i.e., $\mathbb{E}[|h_i|^2] / \mathbb{E}[|h_4|^2] = 10^{\frac{P_i}{10}}$). The variance of the channel path gains are normalized so that the total variance of the channel gains is unity (i.e., $\sum_{i=1}^9 \mathbb{E}[|h_i|^2] = 1$). For the i -th channel path, the Doppler shift is modeled as $\nu_i = \nu_{\max} \cos(\theta_i)$ where $\theta_i, i = 1, 2, \dots, 9$ are i.i.d. uniformly distributed in $[0, 2\pi)$.

In Fig. 3 we plot the PAPR CCDF for the proposed iterative method (“Novel PAPR Encoding scheme”, depicted by green curve) and that of other state-of-art methods for BPSK modulation (i.e., $D = 2$ and $\mathcal{S}_{A,D} = \{A, -A\}$). It is observed that in the absence of any compensation, the PAPR

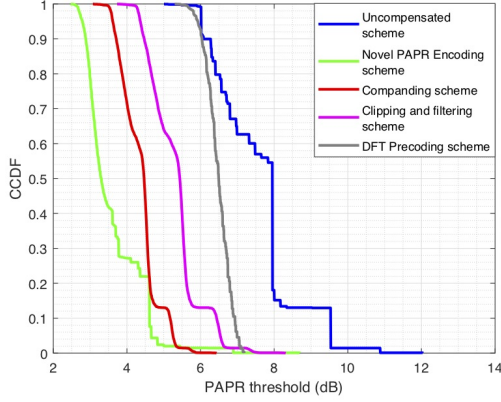


Fig. 3. PAPR CCDF with BPSK.

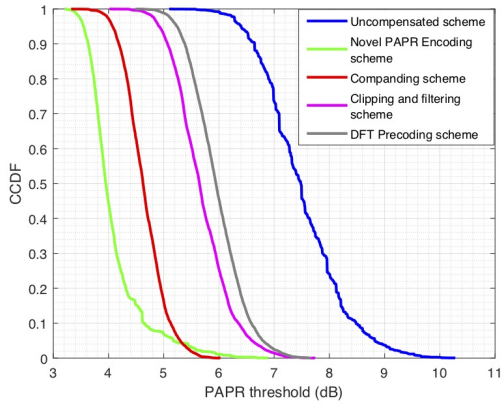


Fig. 4. PAPR CCDF with QPSK.

of an OTFS modulated signal (see the blue curve) can be high as also reported in [16](8 dB for at least half of the random information vectors, i.e., for $CCDF = 0.5$). However, with the proposed method for $CCDF = 0.5$, the PAPR is only around 3.3 dB as compared to 4.5 dB for the companding based method, 5.5 dB for the clipping and filtering based method and 6.5 dB for the DFT-precoding based method.

In Fig. 4 we plot the PAPR CCDF for OTFS modulation with QPSK alphabet (i.e., $D = 4$ and $\mathcal{S}_{A,D} = \{A, A\sqrt{-1}, -A, -A\sqrt{-1}\}$). With QPSK also (just as with BPSK), the PAPR performance of the proposed iterative method is significantly better than that of the other considered methods.

In the proposed PAPR compensation method, the average transmitted power is expected to be higher than that for the uncompensated OTFS transmission, primarily because the precoded symbols may have higher amplitude than that of the information symbols. In the following we therefore study the symbol error rate (SER) performance of the proposed compensation method in comparison with that of uncompensated OTFS and also other considered state-of-art methods.

In Fig. 5 we plot the SER/BER (bit error rate) vs. SNR performance for all methods for OTFS modulation ($M = N = 16$, $\Delta f = 15$ kHz) with BPSK information symbols. The signal-to-noise ratio (SNR) is given by the ratio of the power of

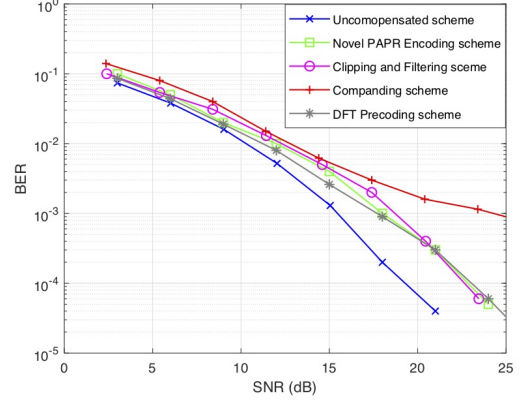


Fig. 5. BER vs. SNR. BPSK information symbols.

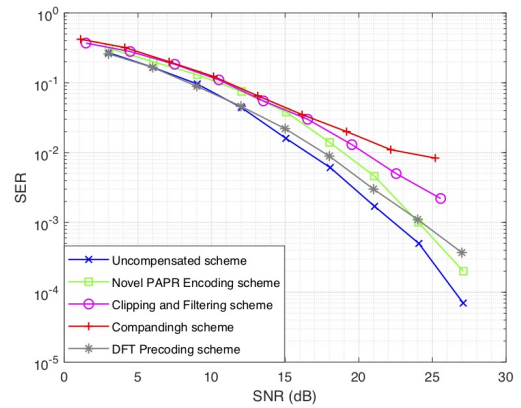


Fig. 6. SER vs. SNR. QPSK information symbols.

the received time-domain signal to the average AWGN power at the receiver (i.e., bandwidth $M\Delta f$ times the AWGN power spectral density). From the figure it is observed that indeed the error rate performance with the proposed PAPR compensation method is slightly inferior to that of uncompensated OTFS modulation. Nevertheless, the error rate performance of the proposed compensation method is similar to that of the DFT precoded and the clipping and filtering based method and is significantly better than that of the companding based method. This fact also holds when the QPSK information symbols are used (see Fig. 6).

In Fig. 7, we plot the QPSK SER for the proposed method and other considered state-of-art methods as a function of increasing path Doppler shift ν_{max} and a fixed SNR of 18 dB. It is observed that the SER performance of the proposed compensation method, the DFT precoded and the clipping and filtering based methods is almost invariant of Doppler shift ($0 \leq \nu_{max} \leq 2400$ Hz) whereas the SER performance of the companding based method degrades with increasing path Doppler shift.

In Table-I we compare the PAPR of all considered methods for CCDF of 0.1 with QPSK symbols, fixed $M = 16$, and varying $N = 4, 8, 16, 32, 64$. It is observed that the proposed method has the smallest PAPR when compared to other methods, for all values of N . The same is valid for

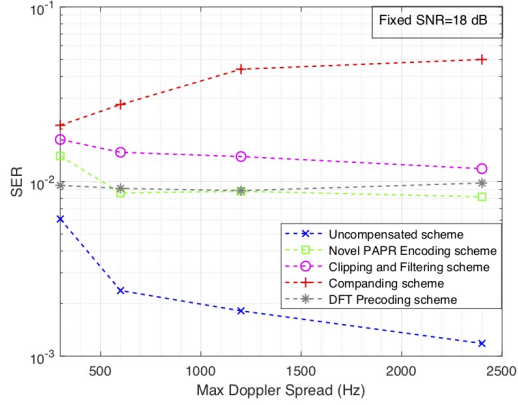


Fig. 7. QPSK SER vs. max. Doppler shift ν_{max} for fixed SNR of 18 dB.

TABLE I
PAPR (dB) FOR CCDF = 0.1, $M = 16$, QPSK

N	Uncompensated scheme	Proposed encoding	Companding scheme	Clipping and Filtering	DFT Precoding
4	6.0	2.8	4.1	4.8	6.2
8	7.8	2.9	4.8	5.9	6.4
16	8.5	3.3	5.2	6.4	6.6
32	9.0	4.0	5.4	6.7	6.8
64	9.6	4.6	5.6	7.2	7.0

fixed $N = 16$ and varying $M = 4, 8, 16, 32, 64$ (see Table-II).

V. CONCLUSION

In this paper, we have proposed a novel PAPR reduction method for OTFS modulation based systems. Numerical simulations reveal that the proposed method results in significant PAPR reduction when compared to an uncompensated OTFS system. Also, the proposed method achieves lower PAPR and has lower compensation complexity than that of the other state-of-art PAPR reduction methods proposed in [18]–[20]. The error rate performance of OTFS systems with the proposed PAPR reduction method is similar to that of other considered state-of-art methods and is invariant for a large range of channel Doppler shifts.

REFERENCES

- [1] "Framework and Overall Objectives of the Future Development of IMT for 2030 and Beyond," Recommendation M.2160-0, International Telecommunication Union (Radiocommunication), Nov. 2023.
- [2] T. Wang, J. G. Proakis, E. Masry and J. R. Zeidler, "Performance Degradation of OFDM Systems Due to Doppler Spreading," *IEEE Trans. on Wireless Commun.*, vol. 5, no. 6, June 2006.
- [3] R. Hadani et al., "Orthogonal Time Frequency Space Modulation," *2017 IEEE Wireless Communications and Networking Conference (WCNC)*, San Francisco, CA, USA, 2017, pp. 1-6.

TABLE II
PAPR (dB) FOR CCDF = 0.1, $N = 16$, QPSK

M	Uncompensated scheme	Proposed encoding	Companding scheme	Clipping and Filtering	DFT Precoding
4	7.8	2.9	4.9	6.0	4.6
8	8.2	3.1	5.0	6.2	6.2
16	8.4	3.3	5.1	6.3	6.7
32	8.8	4.6	5.3	6.5	6.9
64	9.1	5.5	5.5	6.8	7.1

- [4] R. Hadani and A. Monk, "OTFS: A New Generation of Modulation Addressing the Challenges of 5G," arXiv:1802.02623[cs.IT], Feb. 2018.
- [5] S. K. Mohammed, "Derivation of OTFS Modulation From First Principles," in *IEEE Transactions on Vehicular Technology*, vol. 70, no. 8, pp. 7619-7636, Aug. 2021.
- [6] Z. Wei, W. Yuan, S. Li, J. Yuan, G. Bharatula, R. Hadani and L. Hanzo, "Orthogonal Time-Frequency Space Modulation: A Promising Next-Generation Waveform," *IEEE Wireless Communications*, vol. 28, no. 4, pp. 136-144, August 2021.
- [7] P. Raviteja, K. T. Phan, Y. Hong and E. Viterbo, "Interference Cancellation and Iterative Detection for Orthogonal Time Frequency Space Modulation," *IEEE Transactions on Wireless Communications*, vol. 17, no. 10, pp. 6501-6515, Oct. 2018.
- [8] S. Li, W. Yuan, Z. Wei and J. Yuan, "Cross Domain Iterative Detection for Orthogonal Time Frequency Space Modulation," *IEEE Transactions on Wireless Communications*, vol. 21, no. 4, pp. 2227-2242, April 2022.
- [9] W. Yuan, Z. Wei, J. Yuan and D. W. K. Ng, "A Simple Variational Bayes Detector for Orthogonal Time Frequency Space (OTFS) Modulation," *IEEE Trans. on Vehicular Technology*, vol. 69, no. 7, pp. 7976-7980, July 2020.
- [10] W. Shen, L. Dai, J. An, P. Fan and R. W. Heath, "Channel Estimation for Orthogonal Time Frequency Space (OTFS) Massive MIMO," *IEEE Trans. on Signal Processing*, vol. 67, no. 16, pp. 4204-4217, Aug. 2019.
- [11] F. Liu, Z. Yuan, Q. Guo, Z. Wang and P. Sun, "Message Passing-Based Structured Sparse Signal Recovery for Estimation of OTFS Channels With Fractional Doppler Shifts," *IEEE Trans. on Wireless Communications*, vol. 20, no. 12, pp. 7773-7785, Dec. 2021.
- [12] H. B. Mishra, P. Singh, A. K. Prasad and R. Budhiraja, "OTFS Channel Estimation and Data Detection Designs With Superimposed Pilots," *IEEE Trans. on Wireless Commun.*, vol. 21, no. 4, pp. 2258-2274, April 2022.
- [13] I. A. Khan and S. K. Mohammed, "A Low-Complexity OTFS Channel Estimation Method for Fractional Delay-Doppler Scenarios," in *IEEE Wireless Communications Lett.*, vol. 12, no. 9, pp. 1484-1488, Sept. 2023.
- [14] "Best Readings in Orthogonal Time Frequency Space (OTFS) and Delay Doppler Signal Processing," June 2022. <https://www.comsoc.org/publications/best-readings/orthogonal-time-frequency-space-otfs-and-delay-doppler-signal-processing>
- [15] S. C.ripps, "RF Power Amplifiers for Wireless Communications," Artech Publishing House, 1999.
- [16] G. D. Surabhi, R. M. Augustine and A. Chockalingam, "Peak-to-Average Power Ratio of OTFS Modulation," *IEEE Communications Letters*, vol. 23, no. 6, pp. 999-1002, June 2019.
- [17] Y. Rahmatallah and S. Mohan, "Peak-To-Average Power Ratio Reduction in OFDM Systems: A Survey And Taxonomy," *IEEE Communications Surveys & Tutorials*, vol. 15, no. 4, pp. 1567-1592, Fourth Quarter 2013.
- [18] C. Naveen and V. Sudha, "Peak-to-Average Power Ratio reduction in OTFS modulation using companding technique," *2020 5th International Conference on Devices, Circuits and Systems (ICDCS)*, Coimbatore, India, 2020, pp. 140-143.
- [19] Hossain MN, Sugiura Y, Shimamura T, Ryu HG. "DFT-spread OTFS communication system with the reductions of PAPR and nonlinear degradation," *Wireless Personal Commun.* 2020 Dec;115(3):2211-28.
- [20] S. Gao and J. Zheng, "Peak-to-Average Power Ratio Reduction in Pilot-Embedded OTFS Modulation Through Iterative Clipping and Filtering," in *IEEE Commun. Letters*, vol. 24, no. 9, pp. 2055-2059, Sept. 2020.
- [21] P. Raviteja, Y. Hong, E. Viterbo and E. Biglieri, "Practical Pulse-Shaping Waveforms for Reduced-Cyclic-Prefix OTFS," *IEEE Transactions on Vehicular Technology*, vol. 68, no. 1, pp. 957-961, Jan. 2019.
- [22] LTE, "Evolved Universal Terrestrial Radio Access (E-UTRA); Base Station (BS) Radio Transmission and Reception (3GPP TS 36.104 v8.6.0)," ETSI TS, vol. 136, no. 104, July 2009.